

Journal of Materials Chemistry C

Accepted Manuscript



This is an *Accepted Manuscript*, which has been through the Royal Society of Chemistry peer review process and has been accepted for publication.

Accepted Manuscripts are published online shortly after acceptance, before technical editing, formatting and proof reading. Using this free service, authors can make their results available to the community, in citable form, before we publish the edited article. We will replace this *Accepted Manuscript* with the edited and formatted *Advance Article* as soon as it is available.

You can find more information about *Accepted Manuscripts* in the [Information for Authors](#).

Please note that technical editing may introduce minor changes to the text and/or graphics, which may alter content. The journal's standard [Terms & Conditions](#) and the [Ethical guidelines](#) still apply. In no event shall the Royal Society of Chemistry be held responsible for any errors or omissions in this *Accepted Manuscript* or any consequences arising from the use of any information it contains.

AIEgens for real-time naked-eye sensing of hydrazine in solution and on paper substrate: structure-dependent signal output and selectivity

Ruoyu Zhang,^{†a} Chong-Jing Zhang,^{†a} Zhegang Song,^b Jing Liang,^a Ryan Tsz Kin Kwok,^b Ben Zhong Tang,^{b,c} Bin Liu^{*a,d}

Abstract

Paper-based assay is a promising alternative sensing technology due to its portability, low cost and ease of operation compared to solution sensing method. Most of the current fluorophores suffer from aggregation-caused quenching, which affects their signal output in the solid state. Although fluorogens with aggregation-induced emission (AIEgens) have attracted intense research interest for solution assays, they have been rarely employed for solid phase detection due to their high emissivity in aggregated state. In this work, three fluorogens TPE-DCV, MTPE-DCV and NTPE-DCV were designed and synthesized by integration of intramolecular charge transfer and AIE characteristics to fine-tune their absorption and emission maxima. Among the three AIEgens, NTPE-DCV gives the best response to hydrazine, with a detection limit of 143 ppb in solution. In addition, the NTPE-DCV stained paper strip offers fluorescence turn-on from dark to yellow for 1 mM hydrazine solution or 1% hydrazine vapor for naked-eye sensing. It was also found that the fluorogen with stronger electron donor (e.g. NTPE-DCV) showed better selectivity to hydrazine over glutathione. The practical example of hydrazine detection elucidates a general strategy for design of AIE probes that are compatible with both solution and paper-based assays with high sensitivity and rapid signal readout.

Key words:

Paper-based detection; Naked-eye sensing; Aggregation-induced emission (AIE); Intramolecular charge transfer (ICT); Hydrazine detection; Light-up sensing

[a] Ms. Ruoyu Zhang, Dr. Chong-Jing Zhang, Dr. Jing Liang, Prof. Bin Liu
Department of Chemical and Biomolecular Engineering
National University of Singapore
4 Engineering Drive 4, Singapore 117585
E-mail: cheliub@nus.edu.sg

[b] Mr. Zhegang Song, Dr. Ryan Tsz Kin Kwok, Prof. Ben Zhong Tang
Department of Chemistry, Division of Biomedical Engineering,
The Hong Kong University of Science and Technology,
Clear Water Bay, Kowloon, Hong Kong, China

[c] Prof. Ben Zhong Tang
SCUT-HKUST Joint Research Laboratory, Guangdong Innovative Research Team,
State Key Laboratory of Luminescent Materials & Devices,
South China University of Technology,
Guangzhou 510640, China

[d] Prof. Bin Liu
Institute of Materials Research and Engineering (A*STAR)
3 Research Link, Singapore 117602

† These authors contributed equally to this work.

Supporting information for this article is given via a link at the end of the document.

Introduction

Last several decades have witnessed the prosperity of “lab-on-chip”, such as dipstick and lateral-flow assays, which are based on the blotting of the analytes onto a paper pre-stained with probes.^{1,2} The best-known example is pH strips which enable quick colorimetric response to different pH environment. These formats enjoy rapid growth and great popularity due to the good portability, feasible readout and operational simplicity. Common sensors applied on solid-substrate include both colorimetric^{3, 4} and fluorometric formats⁵⁻⁷, which rely on the absorption and emission changes of the signal reporters, respectively. To construct a fluorescence sensing system, fluorophore/quencher pairs are often needed to achieve signal off/on upon reaction with targets. On the other hand, probes which combine the recognition and signaling elements in single molecules simplify the design of sensors significantly.^{8, 9} Creative integration of the reactive sites with latent fluorogens enjoys superiority and versatility for various analytical tasks.¹⁰ The past decades have witnessed the prosperity of detection in solution with the aid of organic fluorogens;¹¹ however, much less examples have been applied to solid-state fluorescent assays, largely due to the detrimental aggregation-caused quenching (ACQ) effect of conventional fluorophores. The decreased fluorescence of the enriched fluorophores on the solid support leads to weakened signal and reduced sensitivity. In addition, due to the intrinsic fluorescence of these fluorophores, additional washing steps are required to remove the excess unbound fluorescent probes. As a consequence, the development of fluorometric probes which are free of ACQ effect is in high demand.

Probes based on fluorogens with aggregation-induced emission characteristics (AIEgen) have attracted intense research interest recently.¹²⁻¹⁵ Opposite to conventional fluorogens suffering from self-quenching, majority of AIEgens show very strong fluorescence in aggregated state or solid state but are almost non-emissive when molecularly dissolved because of the energy consumption of excited states by intramolecular motions.¹⁶⁻¹⁸ Based on this unique optical property, a wealth of fluorescence turn-on AIE probes have been designed for the detection of small molecules, ions and biomacromolecules^{12, 14, 19-28} in solution phase. However, typical AIEgens are not suitable for solid-state light-up detection simply because they exhibit strong fluorescence once deposited on solid substrates, which is difficult to construct turn-on sensors. In order to develop paper-based sensors with good visual contrast and sensitive signal variations in response to analytes, extra strategies are required to manipulate the spectral changes in either intensity or wavelength of the probes. For instance, a maleimide-modified AIE probe was reported for solid-state detection of thiol based on photo-induced electron transfer (PET) mechanism.²⁹ In this work, the maleimide serves as both a fluorescence quencher and the reactive site

for selective addition of thiol. More recently, we reported a light-up probe for detection both in solution and on paper strip based on a salicylaldazine structure.³⁰ The probe shows significant fluorescence enhancement and large Stokes shift which benefits from AIE and excited state intramolecular proton transfer (ESIPT) characteristics, respectively. Although several such examples have been reported, existing AIE platforms which are suitable for paper assays remain limited.

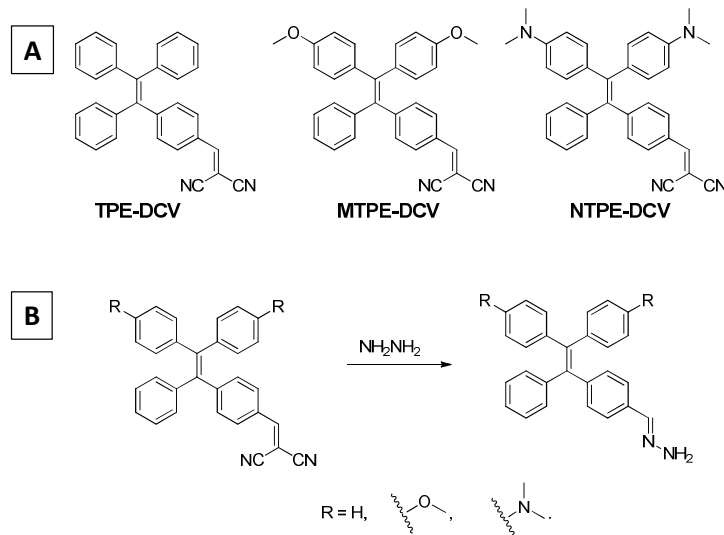
In this contribution, a series of fluorogens suitable for paper assays and free of self-quenching effect were developed by integrating intramolecular charge transfer (ICT) and AIE characteristics. All compounds consist of a strong electron acceptor that not only can extend the absorption and emission peaks to long-wavelength regions, but also is sensitive to nucleophilic targets. Electron-donating groups, such as methoxyl and *N, N*-dimethylamino were introduced to fine-tune the donor-acceptor (D-A) strength, making the fluorogens suitable for naked-eye detection on paper strips. Hydrazine (H₂N–NH₂) was chosen as the model analyte due to its strong nucleophilicity that can break the D-A system and induce changes in the optical properties of the developed fluorogens. In addition, the sensing of hydrazine is of high importance³¹⁻³⁷ as it is a toxic and hazardous environmental pollutant that causes severe damages to human organs and nervous system.³⁸⁻⁴⁰ Upon addition of hydrazine, the probes undergo quick and distinctive spectral changes visible to naked-eye. Furthermore, mechanistic study and selectivity test demonstrate the working principle of the probes and the excellent selectivity over other structural analogs. This work enriches the library of fluorogens suitable for solid-state sensing.

Results and discussion

Probe design and synthesis

The chemical structures of TPE-DCV, MTPE-DCV and NTPE-DCV are shown in Scheme 1A. TPE-DCV contains a typical AIE structure of tetraphenylethylene (TPE) and a dicyanovinyl group as a strong electron acceptor. Efficient ICT process in the compound results in the formation of a new absorption peak at 400 nm as compared to that of TPE.⁴¹ To further fine-tune the intramolecular interaction, electron-donating group, namely methoxyl and *N, N*-dimethylamino group were introduced to the TPE structure to yield MTPE-DCV and NTPE-DCV. The compounds with donor-acceptor (D- π -A) systems are featured with even more red-shifted absorption and emission in the visible region. More importantly, the dicyanovinyl group is reactive to nucleophilic targets such as hydrazine. A general reaction scheme of the probes with hydrazine is provided in Scheme 1B. Reaction with hydrazine will destroy the dicyanovinyl group thus blocking ICT process and altering the intramolecular electron density distribution. This reaction will result in distinguished changes in the UV-vis absorption and fluorescence spectra and enable

colorimetric and fluorometric detection. Once the emission of NTPE-DCV is in the NIR region, the fluorescence is no longer visible to naked eye. Subsequent analyte-induced fluorescence blue-shift will make the assay appear as fluorescence turn-on to human eyes. TPE-DCV, MTPE-DCV and NTPE-DCV were synthesized from their aldehyde-functionalized TPE precursors in the yields of 74%, 85% and 73%, respectively. The ^1H NMR, ^{13}C NMR and HRMS data confirm their right structures. Detailed spectra are shown in the experimental section and supporting information (Figures S1–S4).



Scheme 1. (A) Chemical structures of **TPE-DCV**, **MTPE-DCV** and **NTPE-DCV**; (B) general reaction scheme between the fluorogen and hydrazine.

Optical properties

The UV-visible absorption and PL spectra of the three compounds were measured in DMSO/H₂O (1/99, v/v) as shown in Figure 1. TPE-DCV, MTPE-DCV and NTPE-DCV have two absorption peaks derived from TPE and ICT transition respectively. The absorption peaks from TPE moiety of TPE-DCV, MTPE-DCV and NTPE-DCV are located at 300, 310 and 315 nm while the ICT transitions of the three compounds account for the absorption peaks at 400, 440 and 525 nm, respectively. The ICT absorption bands show an increasingly red-shifted maximum as the substituent group changes from hydrogen to methoxyl group and then to *N,N*-dimethylamino group, resulting in color change from yellow (TPE-DCV and MTPE-DCV) to red (NTPE-DCV). The rationale behind this phenomenon should be ascribed to the increased intramolecular charge transfer effect which results from the variation in the electron donating ability of methoxyl and *N,N*-dimethylamino groups. TPE-DCV and MTPE-DCV show strong yellow and red emission at 570 and 630 nm, respectively. In contrast, NTPE-DCV is only weakly emissive at 760 nm,

and the emission is quenched in very polar media due to its strong charge transfer characteristics. The Stokes shifts increase from 170 nm for TPE-DCV to 190 and 235 nm for MTPE-DCV and NTPE-DCV, respectively, which is beneficial for minimizing interference from the excitation source when used as a probe.

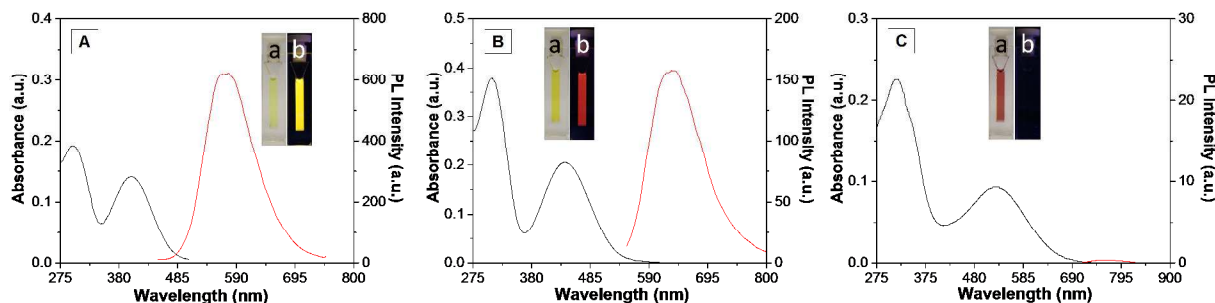


Figure 1. UV-visible absorption (black) and PL spectra (red) of 10 μM (A) TPE-DCV, (B) MTPE-DCV and (C) NTPE-DCV in DMSO/ H_2O = 1/99. λ_{ex} = 400, 440 nm and 525 nm for TPE-DCV, MTPE-DCV and NTPE-DCV, respectively. The insets show photographs of the probes in DMSO/ H_2O mixture (1/99, v/v) under natural (a) and UV light (b).

The AIE characteristics of the three compounds were investigated in detail. The PL intensity of each compound (10 μM) was measured with the water fraction increasing from 0% to 99% in the DMSO- H_2O solvent mixture. As shown in Figure 2A, TPE-DCV remains non-emissive until the water fraction (f_w) goes beyond 40% and its PL intensity at 570 nm experiences a dramatic increase when f_w reaches 50%. Similarly, the PL intensity of MTPE-DCV shows a sudden rise only when f_w reaches 60%. After the dramatic inflection, both TPE-DCV and MTPE-DCV show gradual enhancement in PL intensity with increasing water fractions. In comparison, the PL intensity of NTPE-DCV stays very low and shows a further decreased trend with increasing f_w , and it remains weakly emissive when f_w reaches 99%. The weak fluorescence of NTPE-DCV is attributed to the very strong charge transfer character of the donor-accepter system. The results indicate that TPE-DCV and MTPE-DCV show typical AIE characteristics while the emission of NTPE-DCV is totally extinguished. The spectral nature of NTPE-DCV makes it suitable for development of fluorescence turn-on probes which enjoy low background signal and high signal to noise ratio.

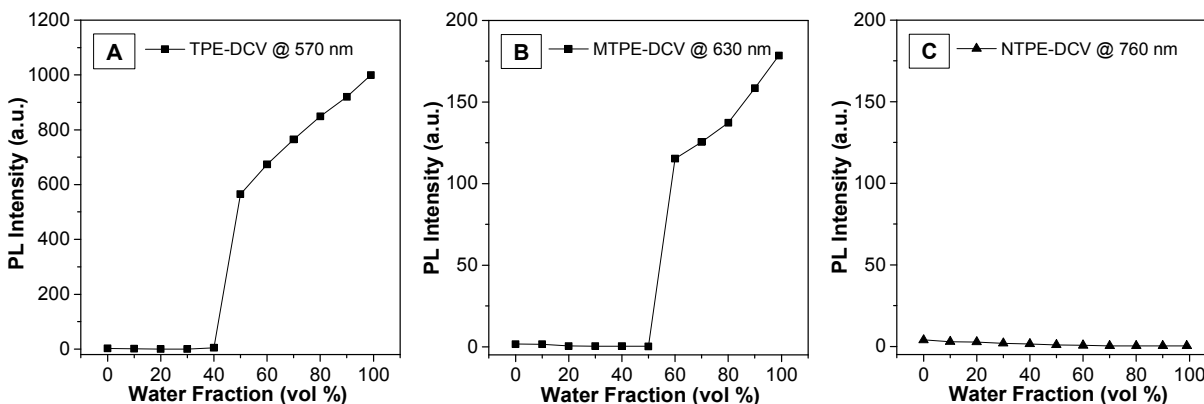


Figure 2. Plots of the maximum PL intensity of 10 μM (A) TPE-DCV, (B) MTPE-DCV, and (C) NTPE-DCV against water fractions (vol %) in the solvent mixture of DMSO- H_2O . $\lambda_{\text{ex}} = 400, 440$ and 525 nm for TPE-DCV, MTPE-DCV, and NTPE-DCV, respectively.

It is known that the emission of AIEgens is closely related to their dispersion status in solution. In general, AIEgens are non-emissive when molecularly dissolved but they become highly emissive when aggregated. Laser light scattering (LLS) was employed to examine the dispersion status of TPE-DCV, MTPE-DCV and NTPE-DCV and the results are presented in Figure 3. TPE-DCV and MTPE-DCV form aggregates with hydrodynamic diameter of 210 and 196 nm, respectively, which is in accordance with the strong emission of the two compounds in aqueous solution. Moreover, NTPE-DCV also forms aggregates with around 200 nm in diameter. The low fluorescence as shown in Figure 2C indicates that NTPE-DCV is not a typical AIEgen by itself.

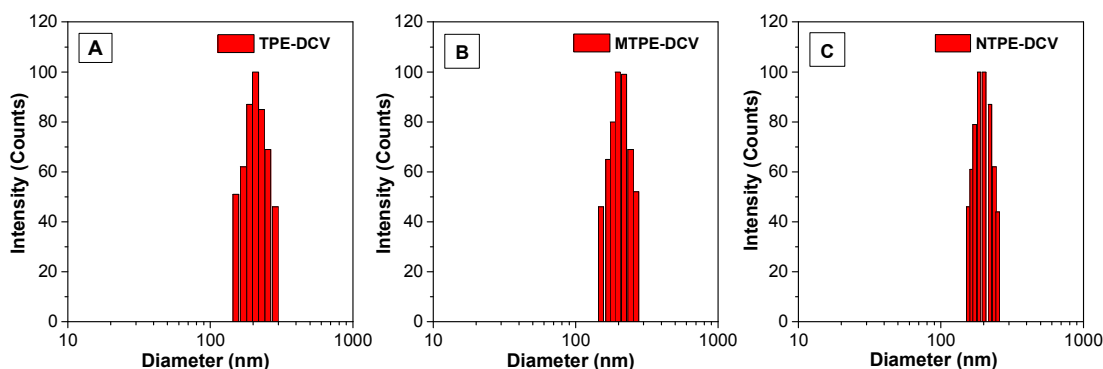


Figure 3. Hydrodynamic diameters of 10 μM (A) TPE-DCV, (B) MTPE-DCV and (C) NTPE-DCV in DMSO/ H_2O ($v/v = 1/99$) measured by LLS.

Spectral responses

To study the potential of the three fluorogens as hydrazine probes, they were first incubated with 1.0 equiv. of hydrazine to yield hydrazone product and then diluted with DMSO/H₂O (v/v = 1/99) for measurement of the spectral changes. As shown in Figure 4, the absorption maxima of TPE-DCV, MTPE-DCV and NTPE-DCV at 400, 440 and 525 nm disappear upon complete reaction and the formation of hydrazone products while new absorption peaks appear at 330, 345, and 380 nm. The probes experienced visible color change from yellow to colorless for TPE-DCV and MTPE-DCV and from red to yellow for NTPE-DCV (insets of Figure 1 and Figure 4). Compared to TPE-DCV and MTPE-DCV, the color change of NTPE-DCV is much more recognizable derived from the significant shift in absorption maximum wavelength from 525 nm to 380 nm upon reaction with hydrazine. Meanwhile, the three fluorogens show evident color changes under UV illumination before and after reaction, as shown in the insets of Figures 1 and 4. The emission maxima of TPE-DCV, MTPE-DCV and NTPE-DCV solutions after reaction are blue-shifted to 490, 515 and 580 nm, respectively, as compared to their original emission spectra in Figure 1. As expected, although NTPE-DCV is almost non-emissive in aqueous solution, it fluoresces strongly at 580 nm after reaction with hydrazine, which makes it an excellent turn-on probe. In fact, the product of NTPE-DCV and hydrazine is an AIEgen (Figure S5), which favors signal output. On the other hand, upon addition of hydrazine, TPE-DCV and MTPE-DCV experienced 80 nm and 115 nm blue-shifts in the emission maxima (Figures 1A, 1B and 4A, 4B), which is a desirable property for ratiometric fluorescence sensing.

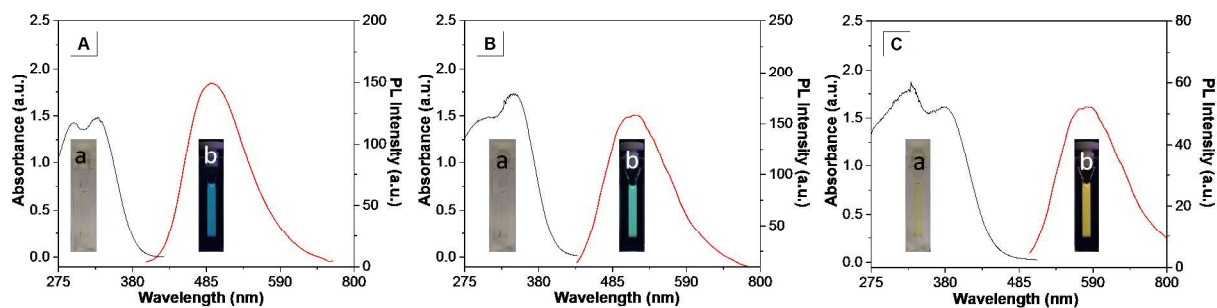


Figure 4. UV-vis absorption (black) and PL (red) spectra of the hydrazone products of (A) TPE-DCV, (B) MTPE-DCV, and (C) NTPE-DCV in DMSO/H₂O (v/v = 1/99). [TPE-DCV] = [MTPE-DCV] = [NTPE-DCV] = 10 μ M. The insets show photographs of hydrazone products under natural (a) and UV light (b).

Hydrazine detection in solution

First, the response time of the probes to hydrazine was investigated using NTPE-DCV as an example. Considering that most environmental and biological detections are conducted in aqueous solution but the probes are highly hydrophobic, mixed solvent containing DMSO/H₂O (v/v = 9/1) solution was chosen as the testing medium. In brief, to 100 μM of NTPE-DCV in DMSO/H₂O mixed solvent, 1.0 and 10.0 equiv. of hydrazine were added and the normalized changes in absorbance over incubation time were recorded and summarized in Figure S6. All three probes respond very quickly to hydrazine and the reaction is neatly completed within 1 min. The spectral responses of TPE-DCV, MTPE-DCV, and NTPE-DCV upon increasing amount of hydrazine were examined subsequently. In the same solvents, the three compounds show blue-shifted absorption maxima of the ICT bands at 390, 425 and 510 nm as compared to those in aqueous media. It should be noted that all compounds exist as molecular species throughout the reaction due to the large fraction of DMSO used. As shown in Figure 5, in the presence of increasing amount of hydrazine, the absorption maxima of the ICT bands for the three probes show evident decrease whereas new absorption peaks at 330, 345 and 380 nm gradually appear for TPE-DCV, MTPE-DCV, and NTPE-DCV with isosbestic points at 356, 380 and 425 nm, respectively. These spectral variations and the visible color changes are clearly recognizable by naked eye (Figure 5 and the insets). The normalized absorption changes against the hydrazine concentrations are plotted in Figure S7, where A_0 and A are denoted as the absorption maxima of the fluorogens in the absence and presence of hydrazine. The normalized changes in absorbance follow a linear trend and reach a maximum when the concentration of hydrazine approaches 1.0 equiv. of the probes. The inset of Figure S7A shows that the linear response range of TPE-DCV towards hydrazine is 16–68 μM with a correlation coefficient of $R^2 = 0.9976$. MTPE-DCV and NTPE-DCV show wider linear response range of 0–60 μM with higher correlation coefficients of $R^2 = 0.9993$ and 0.9994 , as shown in Figures S6B, S6C and the insets, respectively. The limit of detection for the three probes were calculated to be 214, 145 and 143 ppb (hydrazine content) by $(3\sigma/k)$, where σ is the uncertainty of absorbance of the probes and k is the slope of the normalized absorbance over hydrazine concentration. Among the three probes, NTPE-DCV shows the most distinct color change and the most obvious concentration-dependent colorimetric variations from dark red to light yellow as shown in Figure S8, which can be visualized easily by naked-eye.

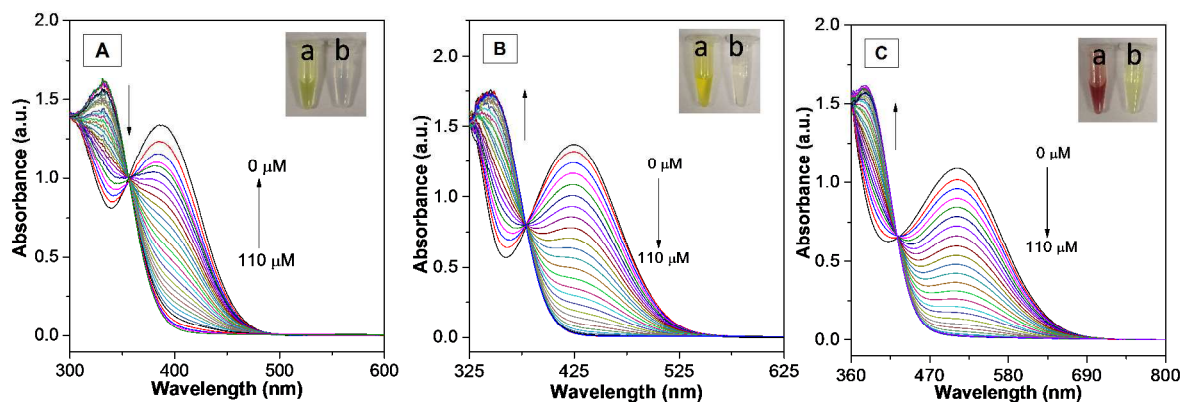


Figure 5. The UV-vis absorption spectra of 100 μM (A) TPE-DCV, (B) MTPE-DCV, and (C) NTPE-DCV against the concentration of hydrazine (0-110 μM) in DMSO-PBS buffer (10 mM, pH = 7.4, 9/1, v/v); the insets are photographs of the probes before and after the reaction with 1.0 equiv. of hydrazine.

The effects of pH on the probe stability and the reaction efficiency with hydrazine were subsequently examined using NTPE-DCV as an example. The UV-vis absorption changes of 100 μM of NTPE-DCV in mixed DMSO-PBS buffer solutions with varying pH values (2–12) of PBS buffer in the absence or presence of hydrazine were recorded. As shown in Figure 6, after incubation with 100 μM of hydrazine for 30 min, NTPE-DCV retains more than 90% absorbance at 510 nm in mixed solutions with pH of PBS buffer varying from 2 to 10. The decreased absorbance of the probe at pH higher than 10 is expected to be arising from the destroyed dicyanovinyl structure and the weakened conjugated system. With the same incubation time, NTPE-DCV exhibits good reactivity towards hydrazine in the pH range of 3–10. The low reaction efficiency at pH 2 is probably because the alkaline hydrazine is neutralized and the probe remains intact at the same pH. It can hence be concluded that NTPE-DCV has a wide working pH range of 3-10 for hydrazine detection, which shows general suitability and better tolerance to acidic or basic conditions compared to previous reports.⁴²⁻⁴⁴ The same trend is also observed for TPE-DCV and MTPE-DCV.

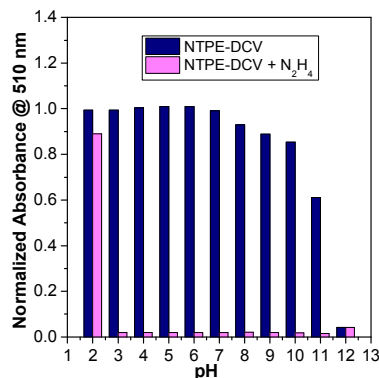


Figure 6. Normalized UV-vis absorbance of NTPE-DCV (100 μ M) at 510 nm in DMSO-PBS buffer mixture (10 mM, 9/1, v/v) at different pH incubated without (navy) and with (magenta) hydrazine (100 μ M) for 30 min.

Sensing of hydrazine on paper strip

After successful demonstration of the colorimetric detection of hydrazine in solution state using the designed fluorogens, we further tested these assays on paper strips. The colorimetric and fluorometric responses of the fluorogens on paper strips were studied and presented in Figure 7. Firstly, 10 μ L of 5.0 mM DMSO stock solutions of TPE-DCV, MTPE-DCV and NTPE-DCV were dropped on filter paper and dried. As shown in the top rows in Figures 7A and 7B, TPE-DCV and MTPE-DCV show light and dark yellow colors under natural light before addition of hydrazine, which fade away upon increasing the concentrations of hydrazine from 10 μ M to 1 M. As shown in the bottom row of Figure 7A, under UV illumination, TPE-DCV shows bright yellow emission, which gradually turns to cyan emission upon formation of hydrazone product with dramatic color change at 10 mM. MTPE-DCV also experienced evident emission color change from bright red to bright blue (bottom row of Figure 7B), which is promising for ratiometric sensing of hydrazine. The color changes under both visible and UV light correlate well with the absorption and emission spectra changes of the probes undergoing reactions with hydrazine in solution.

On the other hand, NTPE-DCV shows purple color by itself under natural light as shown in the top row of Figure 7C. Upon addition of increasing concentrations of hydrazine, the dark purple color of NTPE-DCV fades to light purple and gradually turns to yellow color when hydrazine concentration is increased from 10 μ M to 1 M. It is found that even 10 μ M of hydrazine can induce recognizable color change by naked-eye, which is much more sensitive than TPE-DCV and MTPE-DCV. In addition, NTPE-DCV only shows very weak fluorescence even on the solid substrate as shown in the bottom row in Figure 7C. Upon addition of hydrazine at concentrations from 1 mM, the fluorescence of NTPE-DCV turns

on dramatically, which is at least ten-fold more sensitive than TPE-DCV and MTPE-DCV. Moreover, the combination of the colorimetric and fluorometric changes of NTPE-DCV provides a broad responsive range for visual sensing of hydrazine by naked-eye.

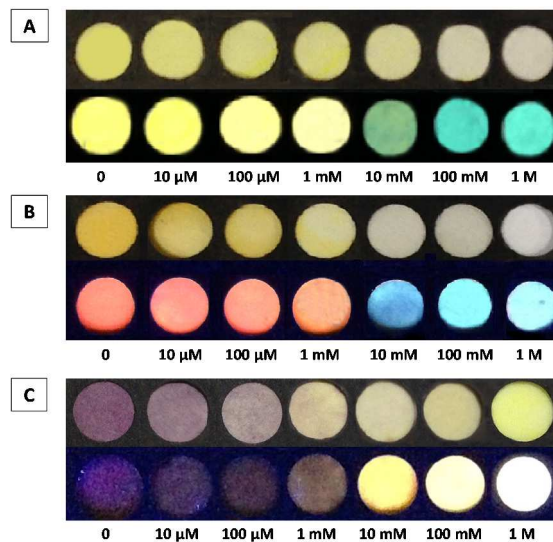


Figure 7. (A) TPE-DCV, (B) MTPE-DCV and (C) NTPE-DCV pre-stained filter paper in the presence of 0 μM , 10 μM , 100 μM , 1 mM, 10 mM, 100 mM, and 1 M of hydrazine. Top row: under visible light; bottom row: under UV light illumination.

NTPE-DCV was subsequently applied for the detection of gaseous hydrazine. A small jar containing hydrazine solution with different concentrations was covered with pre-stained filter paper strips for 10 min at room temperature. Then pictures were taken under natural light (top row) and UV light illumination (bottom row) as shown in Figure 8. The color changes from purple to yellow then to white indicate the increasing concentrations of hydrazine in water from 0% to 50% (v/v). On the other hand, the fluorescence of NTPE-DCV is turned on significantly when the hydrazine concentration reaches 10%. The stained paper strip offers a simple alternative for sensing of gaseous hydrazine, which is potentially useful for hazardous gas detection in case of emergency. It is noteworthy that the fluorescence response to hydrazine vapor is free of self-quenching thanks to its unique AIE characteristics, which is superior to the previous reports.⁴⁵⁻⁴⁶

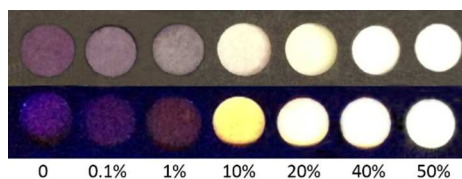


Figure 8. Visual (top) and fluorescent (bottom) color changes of NTPE-DCV stained filter paper after exposure to different concentrations of hydrazine aqueous solution.

Study of selectivity

The selectivity of probes was also tested by measuring the UV-vis absorption changes of NTPE-DCV at 510 nm towards other structurally similar species. As summarized in Figure 9A, NTPE-DCV only shows very minor absorption decrease upon 10 min incubation with 1.0 equiv. of hydrazine analogs including dimethylamine, glutathione (GSH), cysteine, ammonium hydroxide, diethylamine and thiourea. In view of the important biological role of GSH and its existence in high concentration^{41, 47-48}, the response of the three fluorogens towards GSH was studied. Excess amount (1.0 mM) of GSH was incubated with 100 μ M of TPE-DCV, MTPE-DCV and NTPE-DCV, respectively, for 10 min at room temperature. The changes in absorption maxima of each compound were summarized in Figure 9B. NTPE-DCV shows the lowest reactivity to GSH among the three fluorogens. The rationale behind is that the electron-donating substitution exerts negative effects on the nucleophilic addition between the probe and GSH. Nevertheless, as the electron-donating ability of the substituents follows the trend of $-H < -OCH_3 < -N(CH_3)_2$, the electron cloud density at the reactive sites increases in the order of TPE-DCV < MTPE-DCV < NTPE-DCV. This explains why NTPE-DCV shows the lowest reactivity to GSH among the three fluorogens.

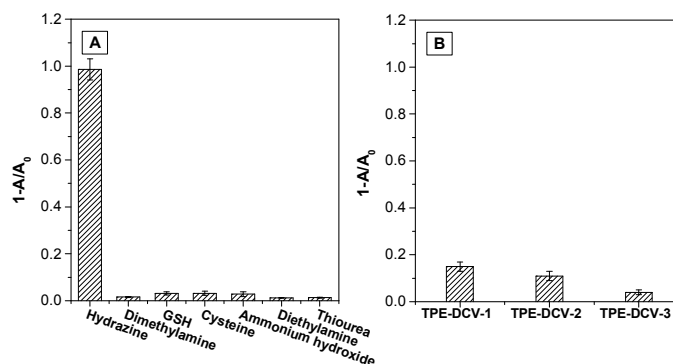


Figure 9. (A) The UV-vis absorption changes of 100 μ M NTPE-DCV incubated with 1.0 equiv. structurally similar analytes to hydrazine for 10 min at room temperature. (B) The UV-vis absorbance changes of 100 μ M TPE-DCV, MTPE-DCV and NTPE-DCV after incubation with 1.0 mM GSH for 10 min. Experiments were conducted in DMSO-PBS buffer (10 mM, pH = 7.4, v/v = 9/1).

Mechanism study

As illustrated above, the reaction between the probes and hydrazine generates the hydrazone group which affects the intramolecular electron density distribution and the optical properties of the probes. Proton NMR spectroscopy and mass spectrometry were further used to confirm the proposed mechanism. Figure 10 shows the ^1H NMR spectra of NTPE-DCV in the absence of hydrazine and after incubation with 0.5, 1.0, and 2.0 equiv. of hydrazine for 10 min to allow for complete reaction. The =CH (a) peak of the dicyanovinyl group at $\delta = 8.7$ ppm (1 H) shifts to 7.6 ppm upon addition of hydrazine, which matches well with the =CH (a') peak of hydrazone product. Besides, the chemical shifts of the aromatic protons b and c of the TPE core also shift from 7.75 ppm to around 6.8 ppm (b' and c'). It can be further proved by the total integration values from 6.3 to 7.3 ppm. Based on the ^1H NMR spectra obtained with varying concentrations of hydrazine from 0.5 to 2.0 equiv., it is concluded that 1 equiv. of hydrazine is required to convert NTPE-DCV fully to the hydrazone product. ESI-MS analysis of the product also reveals the expected peak (Figure S9).

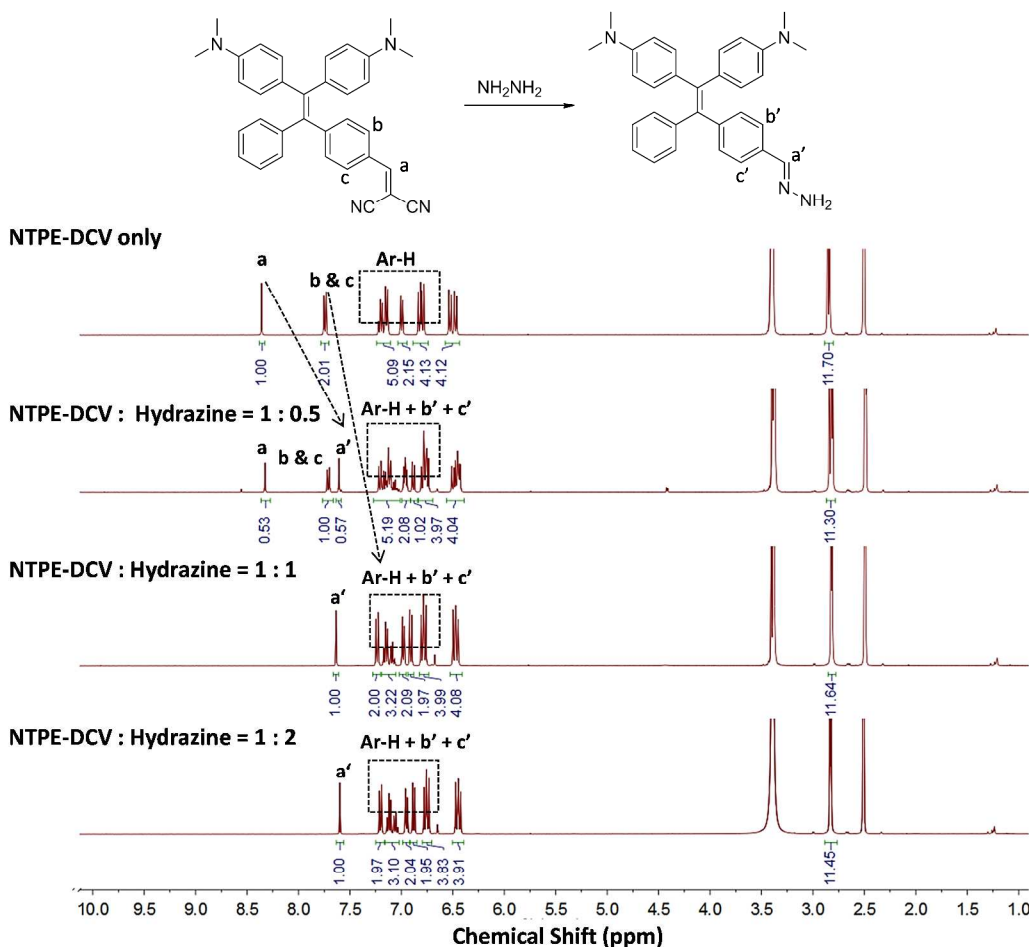


Figure 10. ^1H NMR spectra of NTPE-DCV in the absence and presence of 0.5, 1.0 and 2.0 equiv. of hydrazine after 10 min incubation in $\text{DMSO-d}_6/\text{D}_2\text{O} = 9/1$.

Conclusion

In conclusion, three fluorogens of TPE-DCV, MTPE-DCV and NTPE-DCV were synthesized by integration of ICT and AIE characteristics. The absorption maxima of the probes were tuned from 400 nm to 425 and 510 nm while the emission maxima shift from 570 nm to 630 and 760 nm by changing substituents from hydrogen to dimethoxyl and dimethylamino groups. TPE-DCV and MTPE-DCV generate ratiometric fluorescence response while NTPE-DCV provides remarkable fluorescence turn-on upon addition of hydrazine, which are desirable properties for naked-eye detection and paper assays. The paper assay in this work gives semi-quantitative signal readout and the fluorescence is free of self-quenching effect, which validates a new strategy to apply AIEgens for solid phase detection. Other structurally similar analogs were proved to have little competition with hydrazine, indicating the good selectivity of the probe to hydrazine. What's more, NTPE-DCV was proven to show the best selectivity

among the three to hydrazine against GSH, which is a prevalent species in cancer cells. The platform is desirable for paper assays and enriches the selections of AIEgens for solid-state sensing.

Experimental Section

Materials and Instrumentation

All the chemicals were purchased from Sigma-aldrich or Alfa Aesar and used without further purification. The 10 mM PBS buffer contains 10 mM Na₂HPO₄, 1.8 mM KH₂PO₄, 2.7 mM KCl and 137 mM NaCl. 10 mM PBS buffers with different pH were prepared upon addition of proper amount of NaOH or HCl and were adjusted by a Sartorius basic pH-Meter PB-10. The measurement of UV-vis absorption spectra were carried out on a UV-vis absorption spectrometer (Shimadzu, UV-1700, Japan). PL spectra were collected on a Perkin-Elmer LS-55 equipped with a xenon lamp excitation source and a Hamamatsu (Japan) 928 PMT, using 90° angle detection for solution samples. The size and size distribution of particles were measured by laser light scattering (LLS) with a particle size analyser (90 Plus, Brookhaven Instruments Co., USA) at a fixed angle of 90° at room temperature. ¹H and ¹³C NMR spectra were measured on a Bruker ARX 400 NMR spectrometer. The molecular mass was acquired using ion trap-time-of-flight mass spectrometry (MS-IT-TOF, Shimadzu).

Synthesis and characterization of TPE-DCV, MTPE-DCV and NTPE-DCV

TPE-DCV was synthesized according to the previous report.⁴⁷ MTPE-DCV was prepared from MTPE-CHO, which was first synthesized from MTPE-DCV-Br using 4-bromobenzophenone and 4, 4'-dimethoxybenzophenone as starting materials according to the previous publications. Then to the solution of the MTPE-CHO (87 mg, 0.2 mmol) in dichloromethane (5 mL) was added malononitrile (25 mg, 0.8 mmol) and triethylamine (10 mg, 0.1 mmol). The resulting mixture was stirred at room temperature for 4 h. Then the solvent was removed under reduced pressure. The desired residue was purified with chromatography to yield the product as red solid (79 mg, 85.0%). ¹H NMR (400 MHz, CDCl₃) δ 7.63 (d, *J* = 8.4 Hz, 2H), 7.57 (s, 1H), 7.13–7.16 (m, 5H), 7.01 (m, 2H), 6.92–6.95 (m, 4H), 6.63–6.68 (m, 4H), 3.76 (s, 3H), 3.74 (s, 3H); ¹³C NMR (100 MHz, CDCl₃) δ 159.0, 158.8, 158.6, 152.0, 143.5, 143.1, 137.4, 135.4, 135.3, 132.7, 132.6, 132.5, 131.3, 130.3, 128.5, 128.0, 126.7, 114.1, 113.4, 113.0, 112.9, 80.8, 55.1, 55.0. HRMS (ESI): *m/z* [M + Na]⁺ calcd for C₃₂H₂₄N₂O₂Na: 491.1736; found: 491.1732.

NTPE-CHO was first prepared in a similar way from 4-bromobenzophenone and 4, 4'-Bis(dimethylamino)benzophenone. To the solution of NTPE-CHO (170 mg, 0.4 mmol) in ethanol (8 mL) was added malononitrile (54 mg, 0.8 mmol). The resulting mixture was refluxed for 12 h. Then the solvent was

removed under reduced pressure. The desired residue was purified with chromatography to yield the product as purple solid (143 mg, 72.6%). ^1H NMR (400 MHz, CDCl_3) δ 7.65 (d, $J = 8.8$ Hz, 2H), 7.60 (s, 1H), 7.10–7.16 (m, 5H), 7.04 (m, 2H), 6.90 (d, $J_1 = 8.8$ Hz, $J_2 = 2.0$ Hz, 4H), 6.48 (m, 4H), 2.93 (s, 6H), 2.90 (s, 6H); ^{13}C NMR (100 MHz, CDCl_3) δ 159.1, 153.5, 149.5, 149.2, 145.3, 144.3, 134.9, 132.8, 132.7, 132.6, 131.6, 131.0, 130.3, 127.9, 127.8, 126.1, 114.4, 113.2, 111.3, 111.0, 79.6, 40.2. HRMS (ESI): m/z $[\text{M}+\text{H}]^+$ calcd for $\text{C}_{34}\text{H}_{31}\text{N}_4$: 495.2549; found: 495.2546.

Laser light scattering measurement

30 μL of 1 mM TPE-DCV, MTPE-DCV and NTPE-DCV stock solution in DMSO were diluted to 3 mL H_2O to a final concentration of 10 μM and mixed thoroughly using vortex mixer before LLS measurement using particle size analyser.

Titration of TPE-DCV, MTPE-DCV and NTPE-DCV

1 μL TPE-DCV (10mM in DMSO) was first mixed completely with 999, 899, 799, 699, 599, 499, 399, 299, 199, 99, and 0 μL of DMSO; then to the mixture different amount deionized water were added to yield 1 mL mixture solution with different water fractions (f_w). The PL intensities of each sample were obtained using a Perkin-Elmer LS 55 spectrofluorometer. The titration experiments of MTPD-ECV and NTPE-DCV were carried out in a similar way. $\lambda_{\text{ex}} = 400, 440$ and 525 nm for TPE-DCV, MTPE-DCV, and NTPE-DCV, respectively.

Solution sensing

The UV-vis absorption spectra responsive to hydrazine were measured in the mixture of DMSO-PBS buffer (10 mM, $v/v = 9/1$) with increasing volume of 10 mM hydrazine stock solution in DMSO at the interval of 0.4 μL . After addition of hydrazine solution, the mixture was incubated for 2 min before absorption measurement. The photoluminescence spectra of TPE-DCV, MTPE-DCV and NTPE-DCV as well as their hydrazone products were measured in $\text{DMSO}/\text{H}_2\text{O} = 1/99$. The pH tolerance experiment were carried out in DMSO-PBS buffer (10 mM, $v/v = 9/1$) with varying pH of PBS from 2 to 12. The selectivity of the probes towards other structurally similar analogs was carried out in the mixture of DMSO-PBS buffer (10 mM, $v/v = 9/1$). The probe was first incubated with 1.0 equiv. of analog for 10 min, then the decrease of UV-vis absorption was recorded and normalized.

Paper strip sensing

Whatman filter paper (Advantec, qualitative, 70 mm) was used as the solid substrate for all the solid state sensing. Filter paper strips were stained by 10 μL of 5 mM TPE-DCV, MTPE-DCV and NTPE-DCV

stock solutions in DMSO and dried, respectively. 5 μL of hydrazine solution in methanol with increasing concentrations as described in the figures were then dropped onto the spots and dried in the fame hood for a while before observation and photo-taking.

Vapour gas detection

The above mentioned filter paper was firstly stained by 10 μL of 5 mM NTPE-DCV stock solution in DMSO and dried. Then the probe-loaded paper strips were placed on the top of hydrazine aqueous solution with different concentration in small jars, stayed for 30 min at room temperature and then dried in the fame hood before observation and photo-taking.

Acknowledgements

We thank the Singapore NRF Investigatorship (R-279-000-444-281, R-279-000-444-282), Ministry of Defence (R297-000-340-232), and the SMART (R279-000-378-592), the Research Grants Council of Hong Kong (HKUST2/CRF/10 and N_HKUST620/11) and Guangdong Innovative Research Team Program (201101C0105067115).

Notes and References

1. C. Parolo and A. Merkoçi, *Chem. Soc. Rev.*, 2013, **42**, 450-457.
2. X. Ge, A. M. Asiri, D. Du, W. Wen, S. Wang and Y. Lin, *Trends in Anal. Chem.*, 2014, **58**, 31-39.
3. T.-T. Tsai, S.-W. Shen, C.-M. Cheng and C.-F. Chen, *Sci. Technol. Adv. Mater.*, 2013, **14**, 044404.
4. J. Hu, S. Wang, L. Wang, F. Li, B. Pingguan-Murphy, T. J. Lu and F. Xu, *Biosens. and Bioelectron.*, 2014, **54**, 585-597.
5. E. Petryayeva and W. R. Algar, *Anal. Chem.*, 2013, **85**, 8817-8825.
6. M. O. Noor and U. J. Krull, *Anal. Chem.*, 2013, **85**, 7502-7511.
7. M. O. Noor, A. Shahmuradyan and U. J. Krull, *Anal. Chem.*, 2013, **85**, 1860-1867.
8. X. Li, X. Gao, W. Shi and H. Ma, *Chem. Rev.*, 2014, **114**, 590-659.
9. A. Romieu, *Org. Biomol. Chem.*, 2015, **13**, 1294-1306.
10. M. E. Jun, B. Roy and K. H. Ahn, *Chem. Commun.*, 2011, **47**, 7583-7601.
11. D. Sareen, P. Kaur and K. Singh, *Coord. Chem. Rev.*, 2014, **265**, 125-154.
12. M. Wang, G. Zhang, D. Zhang, D. Zhu and B. Z. Tang, *J. Mater. Chem.*, 2010, **20**, 1858-1867.
13. D. Ding, K. Li, B. Liu and B. Z. Tang, *Acc. Chem. Res.*, 2013, **46**, 2441-2453.
14. R. T. Kwok, C. W. Leung, J. W. Lam and B. Z. Tang, *Chem. Soc. Rev.*, 2014, **43**, 4494-4562.
15. J. Liang, B. Z. Tang and B. Liu, *Chem. Soc. Rev.*, 2015, **44**, 2798-2811.

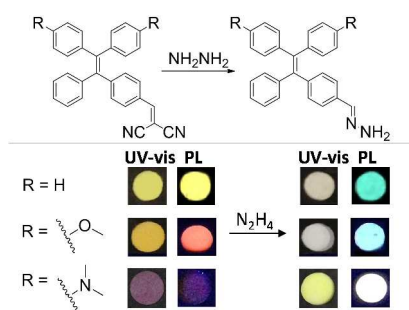
16. Y. Hong, J. W. Y. Lam, and B. Z. Tang, *Chem. Soc. Rev.*, 2011, **40**, 5361-5388.
17. J. Mei, Y. Hong, J. W. Y. Lam, A. Qin, Y. Tang, B. Z. Tang, *Adv. Mater.*, 2014, **26**, 5429-5479.
18. E. P. Parrott, N. Y. Tan, R. Hu, J. A. Zeitler, B. Z. Tang and E. Pickwell-MacPherson, *Mater. Horiz.*, 2014, **1**, 251-258.
19. Y. Yuan, R. T. K. Kwok, G. Feng, J. Liang, J. Geng, B. Z. Tang and Bin Liu, *Chem. Commun.* 2014, **50**, 295-297.
20. X. Wang, J. Hu, G. Zhang and S. Liu, *J. Am. Chem. Soc.*, 2014, **136**, 9890-9893.
21. S. Gui, Y. Huang, F. Hu, Y. Jin, G. Zhang, L. Yan, D. Zhang and R. Zhao, *Anal. Chem.*, 2015, **87**, 1470-1474.
22. X. Chen, L. He, Y. Wang, B. Liu and Y. Tang, *Anal. Chim. Acta.*, 2014, **847**, 55-60.
23. H. Shi, J. Liu, J. Geng, B. Z. Tang and B. Liu, *J. Am. Chem. Soc.*, 2012, **134**, 9569-9572.
24. H. Shi, R. T. K. Kwok, J. Liu, B. Xing, B. Z. Tang and B. Liu, 2012, **134**, 17972-17981.
25. Y. Yuan, R. T. K. Kwok, B. Z. Tang and B. Liu, *J. Am. Chem. Soc.*, 2014, **136**, 2546-2554.
26. Y. Huang, F. Hu, R. Zhao, G. Zhang, H. Yang and D. Zhang, *Chem. – Eur. J.*, 2014, **1**, 158-164.
27. Z. Song, R. T. K. Kwok, E. Zhao, Z. He, Y. Hong, J. W. Y. Lam, B. Liu and B. Z. Tang, *ACS Appl. Mater. Interfaces.*, 2014, **6**, 17245-17254.
28. Y. Wang, Y. Chen, H. Wang, Y. Cheng and X. Zhao, *Anal. Chem.*, 2015, **87**, 5046-5049.
29. Y. Liu, Y. Yu, J. W. Y. Lam, Y. Hong, M. Faisal, W. Z. Yuan, and B. Z. Tang, *Chem. – Eur. J.*, 2010, **16**, 8433-8438.
30. R. Zhang, M. Gao, S. Bai and B. Liu, *J. Mater. Chem. B*, 2015, **3**, 1590-1596.
31. S. Goswami, S. Das, K. Aich, D. Sarkar and T. K. Mondal, *Tetrahedron Lett.*, 2014, **55**, 2695-2699.
32. J. Fan, W. Sun, M. Hu, J. Cao, G. Cheng, H. Dong, K. Song, Y. Liu, S. Sun and X. Peng, *Chem. Comm.*, 2012, **48**, 8117-8119.
33. L. Cui, Z. Peng, C. Ji, J. Huang, D. Huang, J. Ma, S. Zhang, X. Qian and Y. Xu, *Chem. Comm.*, 2014, **50**, 1485-1487.
34. S. Goswami, K. Aich, S. Das, S. B. Roy, B. Pakhira and S. Sarkar, *RSC Adv.*, 2014, **4**, 14210-14214.
35. M. G. Choi, J. Hwang, J. O. Moon, J. Sung and S-K Chang, *Org. Lett.*, 2011, **13**, 5260-5263.
36. C. Hu, W. Sun, J. Cao, P. Gao, J. Wang, J. Fan, F. Song, S. Sun and X. Peng, *Org. Lett.*, 2013, **15**, 4022-4025.
37. S. Goswami, S. Das, K. Aich, B. Pakhira, S. Panja, S. K. Mukherjee and S. Sarkar, *Org. Lett.*, 2013, **15**, 5412-5415.
38. E. H. Vernet, J. D. MacEwen, R. H. Bruner, C. C. Haus and E. R. Kinkead, *Fundam. Appl. Toxicol.*, 1985, **5**, 1050-1064.
39. G. Choudhary and H. Hansen, *Chemosphere*, 1998, **37**, 801.
40. B. K. Sinha and R. P. Mason, *J. Drug Metab. Toxicol.*, 2014, **5**: 168.
41. X. Lou, Y. Hong, S. Chen, C. W. T. Leung, N. Zhao, B. Situ, J. W. Y. Lam and B. Z. Tang, *Sci. Rep.*, 2014, **4**, 4272
42. X.-X. Zhao, J.-F. Zhang, W. Liu, S. Zhou, Z.-Q. Zhou, Y.-H. Xiao, G. Xi, J.-Y. Miao and B.-X. Zhao, *J. Mater. Chem. B*, 2014, **2**, 7344-7350.
43. D.-Y. Qu, J.-L. Chen and B. Di, *Anal. Methods*, 2014, **6**, 4705-4709.

44. M. H. Lee, B. Yoon, J. S. Kim and J. L. Sessler, *Chem. Sci.*, 2013, **4**, 4121-4126.
45. L. Cui, C. Ji, Z. Peng, L. Zhong, C. Zhou, L. Yan, S. Qu, S. Zhang, C. Huang, X. Qian and Y. Xu, *Anal. Chem.*, 2014, **86**, 4611-4617.
46. S. Zhu, W. Lin and L. Yuan, *Anal. Methods*, 2013, **5**, 3450-3453.
47. V. A. Levin, *J. Med. Chem.* 1980, **23**, 682-684.
48. G. Wu, Y. Z. Fang, S. Yang, J. R. Lupton, N. D. Turner, *J. Nutr.* 2004, **134**, 489-492.

**AI-Egens for real-time naked-eye sensing of hydrazine in solution and on paper substrate:
structure-dependent signal output and selectivity**

Ruoyu Zhang,^{†a} Chong-Jing Zhang,^{†a} Zhegang Song,^b Jing Liang,^a Ryan Tsz Kin Kwok,^b Ben Zhong Tang,^{b,c} Bin Liu^{*a,d}

Table of content



AI-Egens for real-time naked-eye sensing of hydrazine in solution and on paper substrate are reported with structure-dependent signal output and selectivity